VOL.39 Nº2 2022
https://doi.org/10.22491/IMECTA.10856.en

Application of the solution blow spinning method to obtain ultra-high-molecular-weight polyethylene (UHMWPE) nanofibers

Karollyne G. C. Monsores*[a], Anderson O. da Silva[b], Ricardo P. Weber[c], Marcos L. Dias[d]
[a, b, c]Instituto Militar de Engenharia, Seção de Engenharia de Materiais – Praça General Tibúrcio, 80, 22290-270, Praia Vermelha, Rio de Janeiro, RJ, Brasil.
[d]Universidade Federal do Rio de Janeiro, Instituto de Macromoléculas Professora Eloíza Mano Av. Horácio Macedo, 2030, 21941-598, Cidade Universitária, Rio de Janeiro, RJ, Brasil.
***karollyne@ime.eb.br**
anderson.q.ao@gmail.com
rpweber@ime.eb.br
mldias@ima.ufrj.br

ABSTRACT: The solution blow spinning (SBS) technique is conceptually similar to electrospinning, but without the application of low currents and high voltage, however with results as satisfactory as for the production of micro and nanofibers. This study aimed to produce ultra-high molecular weight polyethylene (UHMWPE) nanofibers from the SBS technique. SEM images show nanofibers with an average diameter of 200 – 325 nm. The results obtained indicate that the working distance, injection pressure and concentration are variables that directly influence the average fiber diameter, resulting in fibers with smaller diameters for lower concentrations.

KEYWORDS: Ultra-high molecular weight polyethylene. Nanofibers. Solution blow spinning.

RESUMO: A técnica de fiação de solução por sopro (solution blow spinning – SBS) é conceitualmente similar à da eletrofiação (electrospinning), porém sem a aplicação de baixas correntes e de alta tensão, mas com resultados tão satisfatórios quanto para produção de micro e nano fibras. Este estudo objetivou, por meio da técnica SBS, produzir nanofibras de polietileno de ultra alto peso molecular (PEUAPM). As imagens de microscopia eletrônica de varredura (MEV) mostram nanofibras, apresentando diâmetro médio de 200-325 nm. Os resultados obtidos indicam que a distância de trabalho, a pressão de injeção e a concentração são variáveis que influenciam diretamente no diâmetro médio das fibras, resultando em fibras com menores diâmetros para concentrações mais baixas.

PALAVRAS-CHAVE: Polietileno de ultra alto peso molecular. Nanofibras. Fiação de solução por sopro.

1. Introduction

Ultra-high-molecular-weight polyethylene (UHMWPE) is an engineering polymer of increasing industrial production and high performance and economic value. Produced from ethylene gas, similarly to other polyethylene, its macromolecular chain can be 30 times larger than the others. The UHMWPE has a molar mass of $3x10^6$g/mol, with better mechanical response than other polymers of the same class, including: high resistance to impact, abrasion, and chemicals; low coefficient of friction; and high resistance/weight ratio [1,2].

Due to these characteristics, the polymer is mainly applied in harsh or corrosive environments subject to moderate temperatures [2].

However, since UHMWPE presents high viscosity in the molten state, it is difficult to drain at temperatures above the melting point (~135°C) and therefore difficult to process using the conventional methods adopted for thermoplastic polymers [3]. Special processing techniques can be alternatives for UHMWPE, such as compression molding (hot or cold), RAM extrusion, calendering, and gel spinning [4,5].

Despite having limited processing resources, the polymer can be used in various areas of activity,

such as: coatings, in the construction, agricultural, and mining industries; inert artifacts, in the food industry; structural parts, in the beverage, naval, and automotive industry; and mainly in the manufacture of high-performance fibers for high-strength applications and in ballistic shields [4,6].

The conformation of UHMWPE in fibers and/or threads allows both obtaining better mechanical response, mainly attributed to the length/diameter (L/D) ratio of the fiber, and studying new processing media for this and other polymers of high viscosity difficult to process by conventional means. Commercial fibers/membranes of UHMWPE already exist, such as Dyneema®, produced by polymer gel spinning [7,8], Tensylon®, by solid state extrusion [9,10], and Spectra®, by spinning process [11,12].

The advent of nanotechnology has increased the interest of science on the production of polymer nanofibers regarding their potential high-performance applications, attributed to the high specific surface area (area/unit of mass) and the aspect ratio, as shown in macroscopic fibers. On a commercial scale, these fibers are currently made by electrospinning, facing challenges such as high productivity and effective cost [13-15]. The electrospinning technique consists of applying a high-voltage electric field to a syringe containing the polymeric solution. After overcoming the surface tension, a thin jet is directed to the collector where the nanofibers are deposited. The fibers obtained by this method are greatly influenced by the physical-chemical variables of the solutions used, including viscosity, dielectric potential, needle to collector distance, environmental factors, etc. These variables affect the morphology and thickness of the fibers. The influence of other factors, including the chemical composition of both polymer and solvent, molecular weight and molecular weight distribution, and concentration of solutions, among others, on the fibers generated can vary [16-18]. However, since the commercial scalability of the fibers is still low, new processing routes have been investigated, such as the Solution Blow Spinning (SBS) system [19].

The SBS method is considered efficient to largely produce fine fibers since, unlike electrospinning, it requires no electric field to direct the fibers to the collector. The SBS system consists of a gas/air source equipped with a pressure regulator, a syringe pump, a spray machine, and a collector [19]. In the system, a high-pressure flow created from a controlled injection of compressed air stretches the fibers. The polymer solution is blown towards the collection target and the fibers are generated during solvent evaporation within the working distance between the injection nozzle and the collector [19,20].

Fig. 1 presents two schemes of the electrospinning and solution blow spinning systems.

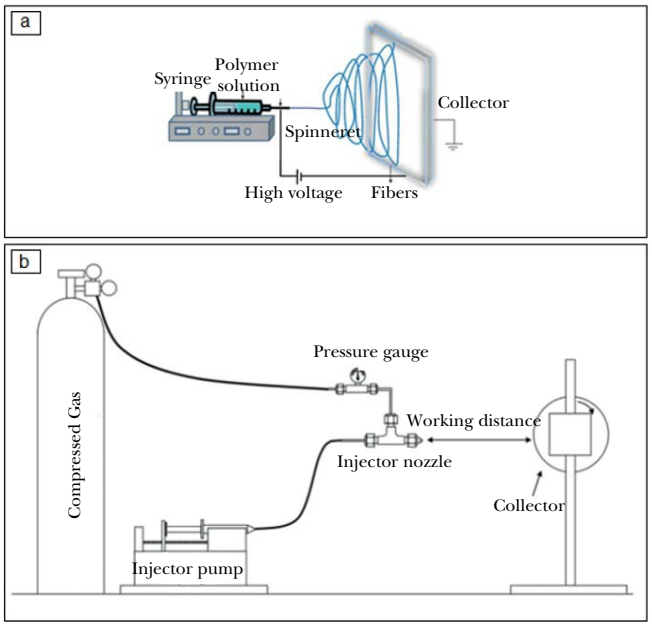

Fig. 1 – Schematic representations of electrospinning (a) and solution blow spinning (b) systems. **Source: Adapted from [19, 21].**

SBS also presents some parameters and process variables that influence the shape of the polymer jet produced, including the molecular weight, concentration, and viscosity of the polymer solution

and the gas pressure and flow rate of the solution — thus affecting the final product [22]. The study of Silva *et al*. [23] to obtain PVC nanofibers by SBS showed that the average fiber diameter is directly proportional to the polymer concentration in the solvent, corroborating previous studies [24-26]. Simultaneously, in another study the average fiber diameter tends to decrease with a lower viscosity of the polymer solution [27]. According to the study, this behavior is associated with greater chain mobility.

The literature has incipient evidence on these parameters and trends for polymeric materials of high molecular weight and therefore high viscosity, such as UHMWPE.

Among the processing variables in SBS, processing temperature stands out, commonly corresponding to room temperature (~31°C). UHMWPE, however, maintains gel form at temperatures from 120°C. Adjusting processing temperature according to the polymer used — such as UHMWPE and others — thus allows controlling the viscosity and solubility of the polymer.

Therefore, considering the high production rate of the SBS system and the difficulty to process UHMWPE by conventional means, this study aimed to produce ultra-high-molecular-weight polyethylene nanofibers using the Solution Blow Spinning system, assessing the effect of spinning conditions on fiber morphology and diameter. Processing was validated by scanning electron microscopy (SEM-FEG).

2. Materials and methods

To design this study, samples of commercial UHMWPE, MIPELON® PM-200 from Mitsui Chemicals were used in powder form ranging from 10 µm to 30 µm diameter. Table 1 shows the values of UHMWPE properties provided by the company.

Table 1 – Properties of MIPELON® commercial UHMWPE.

MIPELON®			
Properties	**Method**	**Unit**	**Value**
Mean Molar Mass	Internal	10^6 g/mol	1.8
Density	ASTM D-1505	g/cm³	0.940
Tensile strength	ASTM D-638	Mpa	≥ 44
Elongation at break	ASTM D-638	%	> 350
Melting temperature	ASTM D-2117	°C	136

Source: [28].

Fig. 2 presents a schematic design of the system adapted from SBS to obtain UHMWPE nanofibers. Unlike in Fig. 1b, the system assembled to obtain nanofibers in this work has a heating system in the reservoir and in the injection nozzle containing the polymer/solvent solution.

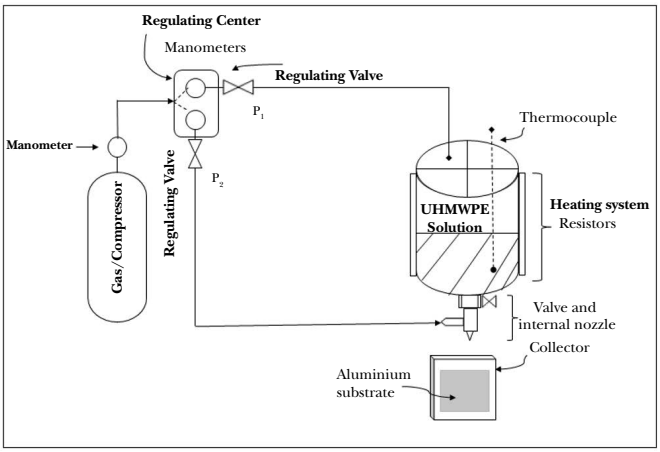

Fig. 2 – Schematic representation of the SBS system used to obtain UHMWPE nanofibers.

For the solubilization of MIPELON® UHMWPE, the p-Xylene solvent was used. To verify the influence of the solution concentration and viscosity in obtaining the nanofibers, the solution concentration used ranged from 0.01 to 0.04% in polymer weight. The UHMWPE/Xylene set was pre-mixed into a heater plate with magnetic agitation at 130°C.

This gel solution was added to the reservoir of the experimental device, heated to controlled temperature (120–135°C). To obtain the nanofibers, the injection nozzle used included metal concentric needles of about 0.03 and 0.05 mm. A heating system ranging from 90 to 150°C was adopted on the needles to avoid clogging the injection nozzle and help evaporate the solvent contained in the solution as soon as the latter was blown against the collector. An injection pressure was applied to the nozzle, ranging from 40 to 60 Psi. The needle to fixed collector distance varied from 15 to 30 cm. The process was conducted under the environmental conditions of ~25°C temperature and 55% of relative humidity. The nanofibers were deposited in an aluminum substrate with 30 × 30 cm dimensions, forming non-woven fabric (NWF) membranes (Fig. 3).

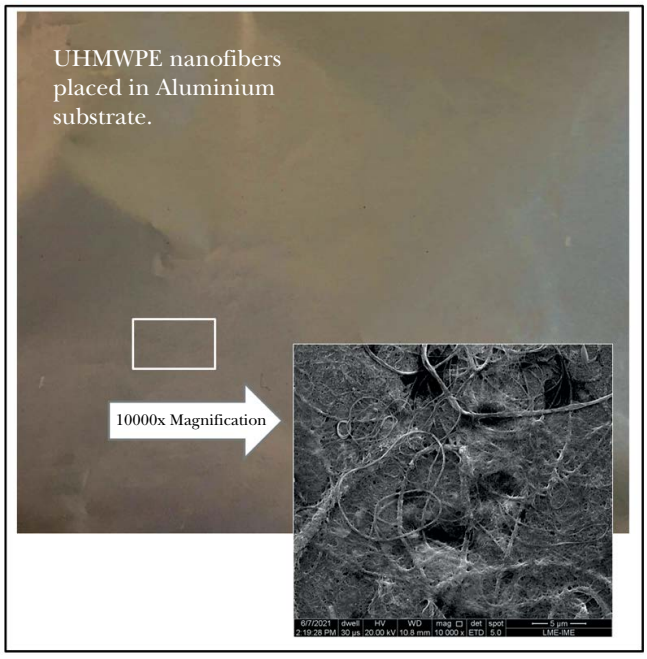

Fig. 3 – Photograph of a membrane of non-woven fibers, spun by solution blow and collected in a fixed collector of 30 × 30cm.

Table 2 shows the different evaluation groups studied considering the variables adopted (concentration, pressure, and working distance) for better conditions of UHMWPE processing by SBS.

The morphology of UHMWPE nanofibers was assessed under an FEG scanning electron microscope, SEM-FEG, operated at 10 kv voltage. The ImageJ software was used to determine the average diameter of the nanofibers. For each evaluation group studied, 50 diameter measurements were taken.

To verify the presence of significant differences between the average diameter of each evaluated group, the Kruskal-Wallis statistical analyses and Dunn's multiple comparisons test were performed. This allowed identifying the statistical significance of these values for a given confidence level since p-values equal to or greater than α (0.05% test significance level) indicate that the study variables are not statistically significant.

Table 2 – Evaluation groups.

GROUPS	CONDITIONS
A	0.01 m/v% UHMWPE, 40 Psi, and 30 cm from the collector.
B	0.03 m/v% UHMWPE, 40 Psi, and 30 cm from the collector.
C	0.04 m/v% UHMWPE, 40 Psi, and 30 cm from the collector.
D	0.01 m/v% UHMWPE, 50 Psi, and 30 cm from the collector.
E	0.01 m/v% UHMWPE, 40 Psi, and 15 cm from the collector.
F	0.01 m/v% UHMWPE, 50 Psi, and 15 cm of the collector.

3. Results and discussion

3.1 Influence of concentration

UHMWPE nanofibers were obtained by SBS using three different concentrations: 0.01%, 0.03%, and 0.04% m/v. A 30 cm distance from the collector and 40 Psi injection pressure were applied to assess the morphology and average diameter of the fibers obtained by the spinning method as a function of the concentrations used. Figs. 4, 5, and 6 present the photomicrographs and their respective average diameter distribution curves for concentrations 0.01%, 0.03%, and 0.04%.

For the three concentrations studied, fibers had no pores or beads, presenting constant diameter along their length. However, we observed a complex structure formed by fibers with two dimensional levels: micro and nano.

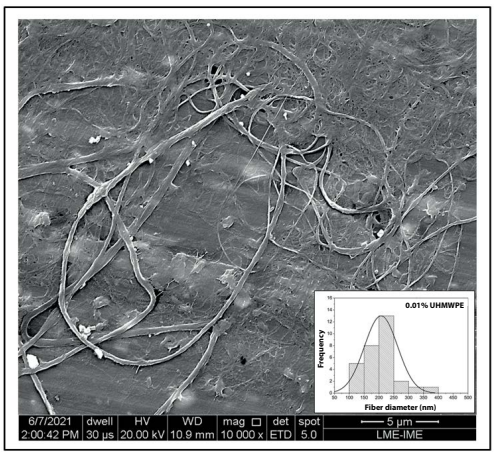

Fig. 4 – Morphology and distribution curve of fibers obtained from condition A. Concentration of 0.01% m/v, 40 Psi injection pressure, and 30 cm distance from fixed collector.

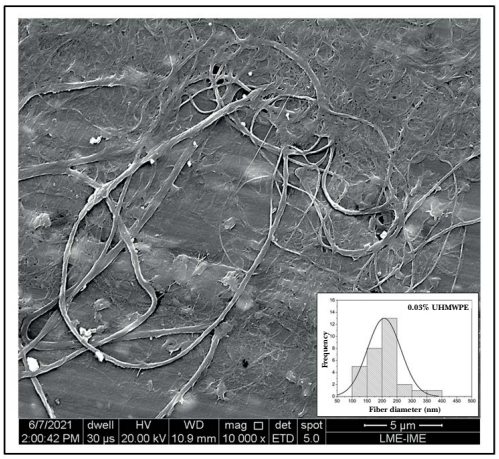

Fig. 5 – Morphology and distribution curve of fibers obtained from condition B. Concentration of 0.03% m/v, 40 Psi injection pressure, and 30 cm distance from fixed collector.

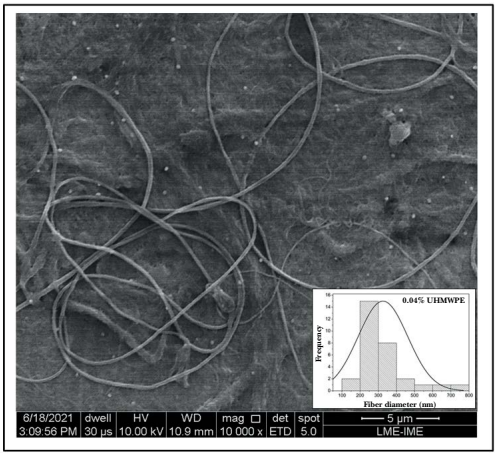

Fig. 6 – Morphology and distribution curve of fibers obtained from condition A. Concentration of 0.04% m/v, 40 Psi injection pressure, and 30 cm distance from fixed collector.

In the literature, several researchers [19,29,30] have reported this result. The distribution of fibers for the SBS technique was more uneven than for the electrospinning technique. This suggests that fiber bundles are more likely to form from the supply of a minimum solution quantity, as seen by the greater diameter distribution in concentration 0.01% m/v. This behavior could also occur due to the turbulence produced by the air jet around the gel-spun solution, forming several bundles of gel solution that come out of a single nozzle and intersect in the air, producing bundles of fibers before the solvent completely evaporates [22]. The morphologies obtained are similar to the visual pattern of UHMWPE nanofibers obtained via electrospinning [31-33].

Table 3 shows the average diameter found for each of the conditions. Average diameter progressively increased with concentration, being 5% for the concentration of 0.03% m/v (p-value 6.65×10^{-01}) and 64% for the concentration of 0.04% m/v (p-value 3.96×10^{-7}) when compared to the concentration of 0.01%. This could be associated with increased viscosity of the solutions used since the increase in the viscosity of the polymer/solvent mixtures contributes to uniformity, increasing fiber diameter [34,35].

However, results show that from concentration 0.03% m/v the increase in polymer/solvent concentration greatly influences the diameter of the spun fibers of UHMWPE, almost doubling the value obtained in condition A.

Table 3 – Average diameters obtained from conditions A, B, C. Injection pressure 40 Psi and distance from collector 30 cm.

Group	Concentration (%m/v)	Average diameter (nm)
A	0.01	199.66 ± 60.13
B	0.03	207.86 ± 55.82
C	0.04	325.90 ± 136.27

3.2 Influence of injection pressure

As aforementioned, the literature proposes that injection pressure is one of the processing variables which monitors the average diameter of fibers and their distribution due to the orientation imposed on the jet trajectory, the stability of the Taylor cone formed and, mainly, the area of fiber deposition [36,37]. The effect of injection pressure on morphology and distribution of average diameters was investigated from the previous concentration, 0.01% m/v of UHMWPE, which had the lowest diameter values. To assess the influence of this processing parameter, a 30 cm distance from collector was set and the pressure varied from 40 Psi to 50 Psi. Fig. 7 presents the photomicrographs and their respective distribution curves of average diameter for the injection pressure of 50 Psi and Tab. 4 reports the measured diameter values for each of the conditions.

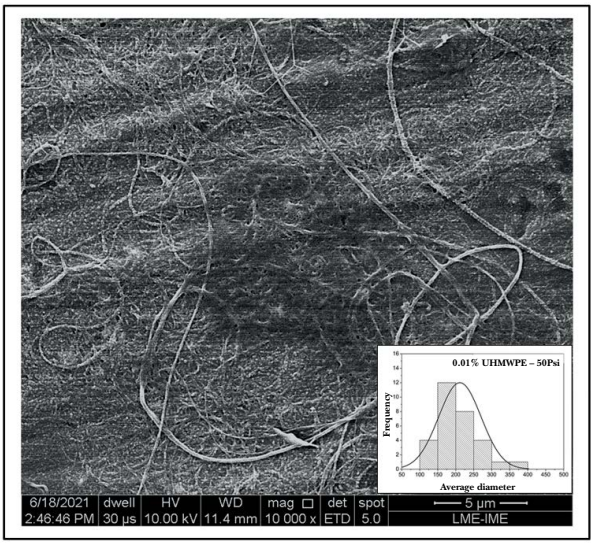

Fig. 7 – Morphology and distribution curve of fibers obtained from condition D. Concentration of 0.01% m/v, 50 Psi injection pressure, and 30 cm distance from fixed collector.

Table 4 – Average diameters obtained from conditions A and D. Concentration 0.01% wt and distance from collector 30 cm.

Group	Concentration (%m/v)	Pressure (Psi)	Average diameter (nm)
A	0.01	40	199.66 ± 60.13
D	0.01	50	211.51 ± 58.77

For the SBS technique, the air injection pressure should exceed the surface tension of the polymer solution, lengthening it into ultrafine fibers [38–40]. The fibers obtained with injection pressure of 50 Psi increased 6% in average diameter compared to those obtained with 40 Psi (p-value 3.86×10^{-01}). High air flows create fibers with larger diameters since the fiber bundles are delivered to the collector at high speed, hindering the complete volatilization of the solvent. In turn, low air flows produce no fibers or smaller diameter fibers since they must achieve the force needed to break the surface tension of the solution. This phenomenon was observed for PLA, PTFE, PEO, PCLA, Nylon 6, among others [38,41-44]. Higher injection pressures thus require longer deposition distances between the needle tip and the collector to avoid this phenomenon.

3.3 Influence of distance from collector

The effect of the distance from the collector on the morphology and distribution of average diameters was investigated by establishing a 0.01% m/v concentration and a 15 cm distance from the collector. The results obtained were compared with those presented in the previous section. Figs. 8a and 8b present the photomicrographs and their respective distribution curves for the injection pressures of (a) 40 Psi and (b) 50 Psi and Tab. 5 reports the measured diameter values for each of the conditions.

The optimal working distance is understood in the balance between the minimum distance required to collect the fibers completely dry and a maximum distance without excessive loss of the material, thus producing more fibers with smaller diameters [45]. Working distance showed no significant change in the average diameter or morphology obtained for the injection pressure of 50 Psi (p-value 5.87×10^{-01}), likely since the deposition speed was very high. For 40 Psi pressure, in turn, the variable increased the average diameter by 44%, modifying size distribution and fiber dispersion (p-value 8.33×10^{-05}).

A too short working distance does not allow the fibers to sufficiently elongate or the solvent

to evaporate completely, thus producing larger diameter fibers and reducing the area of fiber deposition and dispersion [19,46].

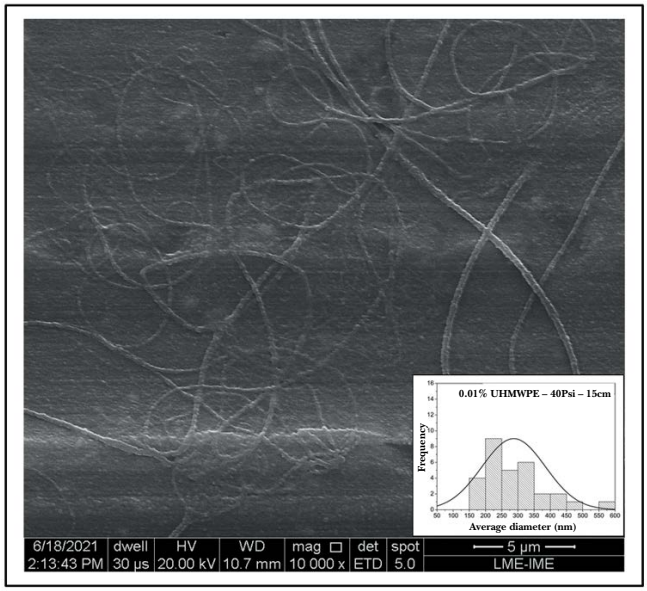

Fig. 8a – Morphology and distribution curve of fibers obtained from condition E. Concentration of 0.01% m/v, 40 Psi injection pressure, and 15 cm distance from fixed collector.

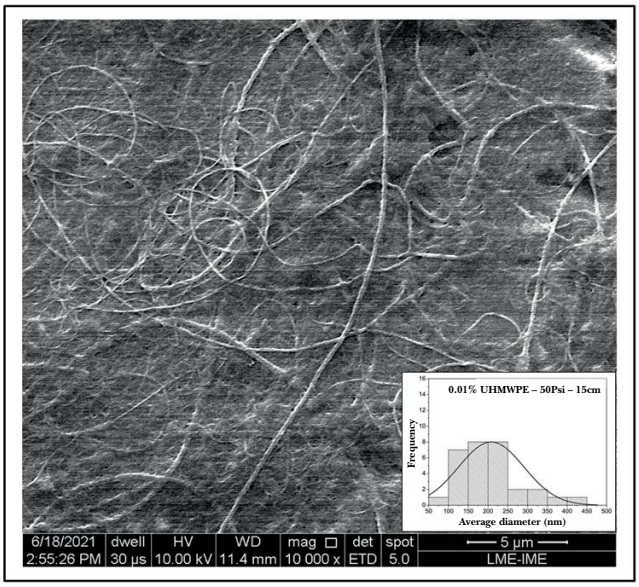

Fig. 8b – Morphology and distribution curve of fibers obtained from condition E. Concentration of 0.01% m/v, 50 Psi injection pressure, and 15 cm distance from fixed collector.

Table 5 - Average diameters obtained from conditions E and F. Concentration 0.01% m/v and distance from collector 15 cm.

Group	Concentration (%m/v)	Pressure (Psi)	Collector distance (cm)	Average diameter (nm)
E	0.01	40	15	287.01 ± 97.74
F	0.01	50	15	208.24 ± 82.46

3.5 Statistical evaluation

The Kruskal Wallis nonparametric statistical analysis showed that for all variables studied (concentration, air pressure, and distance from collector) in the processing of UHMWPE nanofibers, the response variable (average diameter) presents a statistical difference indicated by $p = 6.20 \times 10^{-9}$ for the significance level of 0.05%. To specifically identify which conditions presented differences, Dunn's multiple comparisons test was used. Table 6 presents the estimated values and the combinations that differ statistically were highlighted in gray.

Table 6 – Results of multiple comparisons obtained by Dunn's test.

Comparisons	p-value
A-B	6.65×10^{-01}
A-C	3.96×10^{-07}
A-D	3.86×10^{-01}
A-E	8.33×10^{-05}
A-F	7.46×10^{-01}
B-C	3.53×10^{-06}
B-D	6.65×10^{-01}
B-E	4.64×10^{-04}
B-F	9.12×10^{-01}
C-D	2.63×10^{-05}
C-E	2.56×10^{-01}
C-F	2.06×10^{-06}
D-E	2.16×10^{-03}
D-F	5.87×10^{-01}
E-F	3.05×10^{-04}

4. Conclusion

Assessment of the experimental results obtained and of information in the literature indicates that in processing by solution blow spinning, UHMWPE

is influenced by solution concentration, injection pressure, and working distance, affecting morphology and average diameter distribution.

- For the three concentrations studied, 0.01% m/v presented the lowest mean fiber diameter.
- Regarding injection pressure, the smaller air flows produced fibers with smaller diameters, depending on the distance between the needle tip and the fixed collector.
- Working distance mainly affected the dispersion of the fibers processed, showing no change for the pressure of 50 Psi.
- Condition A was the processing condition with the smallest average fiber diameter, with 199.66 ± 60.13 nm.

The fiber formation conditions in this spinning method are physical agents, such as the type of polymer, concentration, injection pressure and, therefore, the morphology and average diameter of the fibers. Conducting statistical and experimental analyses, as done in this study, allows reaching an ideal condition for the UHMWPE/Xylene system, which guarantees that limits of spinning capacity will be reached, increasing production and reducing undesirable effects – always analyzing the effect of parameters in a combined way since experimental variables interact with each other.

Acknowledgments

The authors would like to thank the Brazilian agencies Coordination of Higher Education Personnel (Capes), the National Council for Scientific and Technological Development (CNPq), and the Carlos Chagas Filho Foundation for Research Support of the State of Rio de Janeiro (Faperj) for funding this study.

References

[1] SOBIERAJ, M. C.; RIMNAC, C. M. Ultra high molecular weight polyethylene: Mechanics, morphology, and clinical behavior. Journal of the Mechanical Behavior of Biomedical Materials, v. 2, n. 5, p. 433–443, 2009. https://doi.org/10.1016/j.jmbbm.2008.12.006.

[2] COUTINHO, F. M. B.; MELLO, I. L.; SANTA MARIA, L. C. Polietileno: principais tipos, propriedades e aplicações. Polímeros, v. 13, n. 1, p. 1–13, 2003. https://doi.org/10.1590/S0104-14282003000100005.

[3] KURTZ, S. M. The UHMWPE Handbook. Amsterdam: Elsevier, 2004.

[4] BRASKEM. Polietileno de Ultra-Alto Peso Molecular (PEUAPM). Catálogo Prod UTEC 2015.

[5] AGUIAR, V. O.; PITA, V. J. R. R.; MARQUES, M. F. V. Nanocomposites of ultrahigh molar mass polyethylene and modified carbon nanotubes. Journal of Applied Polymer Science, v. 136, n. 19, p. 47459, 2019. https://doi.org/10.1002/app.47459.

[6] ALVES, A. L. S.; NASCIMENTO, L. F. C.; MIGUEZ SUAREZ, J. C. Comportamento balístico de compósito de polietileno de altíssimo peso molecular: efeito da radiação gama. Polímeros, v. 14, n. 2, p. 105–111, 2004. https://doi.org/10.1590/S0104-14282004000200014.

[7] MARISSEN, R. Design with Ultra Strong Polyethylene Fibers. Materials Sciences and Applications, v. 2, n. 5, p. 319–330, 2011. https://doi.org/10.4236/msa.2011.25042.

[8] PEIJS, T.; JACOBS, M. J. N.; LEMSTRA, P. J. High Performance Polyethylene Fibers. In CHOU, T. W.; KELLY, A.; ZWEBEN, C. Comprehensive composite materials, 1. Amsterdam: Elsevier, 2000. p. 263–301.

[9] DUPONT. Polyethylene sheet and articles made therefrom 2021.

[10] DUPONT. Materiais de alta performance. [2014]. Disponível em: https://www.dupont.com.br/products/tensylon.html. Acesso em: 8 set. 2021.

[11] BHATNAGAR, A.; BRIAN, D. A.; TAN, C. B. C.; WAGNER, L. L. Enhanced ballistic Performance of Polymer Fibers, 2011.

[12] HONEYWELL. SPECTRA FIBER. Products. 2020. Disponível em: https://industrial.honeywell.com/us/en/applications/cut-resistant-fibers-and-materials/rope/spectra-fiber. Acesso em: 8 set. 2021.

[13] MERCANTE, L. A.; ANDRE, R. S.; MACEDO, J. B.; PAVINATTO, A.; CORREA, D. S. Nanofibras Eletrofiadas e suas Aplicações: Avanços na Última Década. Química Nova, v. 44, n. 6, p. 717–36, 2021. https://doi.org/10.21577/0100-4042.20170721.

[14] JAYARAMAN, K.; KOTAKI, M.; ZHANG, Y.; MO, X.; RAMAKRISHNA, S. Avanços recentes em nanofibras de polímero. Journal of Nanoscience and Nanotechnology, v. 12, n. 1-2, p. 52–65, 2004. https://doi.org/doi:10.1166/jnn.2004.078.

[15] STOJANOVSKA, E.; CANBAY, E.; PAMPAL, E. S.; CALISIR, M. D.; AGMA, O.; POLAT, Y. et al. A review on non-electro nanofibre spinning techniques. RSC Advances, v. 6, n. 87, p. 83783–83801, 2016. https://doi.org/10.1039/c6ra16986d.

[16] BEACHLEY, V.; WEN, X. Effect of electrospinning parameters on the nanofiber diameter and length. Materials Science and Engineering: C, v. 29, n. 3, p. 663–668, 2009. https://doi.org/10.1016/j.msec.2008.10.037.

[17] BUTTAFOCO, L.; KOLKMAN, N. G.; ENGBERS-BUIJTENHUIJS, P.; POOT, A. A.; DIJKSTRA, P. J.; VERMES, I. et al. Electrospinning of collagen and elastin for tissue engineering applications. Biomaterials, v. 27, n. 5, p. 724–734, 2006. https://doi.org/10.1016/j.biomaterials.2005.06.024.

[18] MIRJALILI, M.; ZOHOORI, S. Review for application of electrospinning and electrospun nanofibers technology in textile industry. Journal of Nanostructure in Chemistry, v. 6, p. 207–213, 2016. https://doi.org/10.1007/s40097-016-0189-y.

[19] MEDEIROS, E. S.; GLENN, G. M.; KLAMCZYNSKI, A. P.; ORTS, W. J.; MATTOSO, L. H. C. Solution blow spinning: A new method to produce micro- and nanofibers from polymer solutions. Journal of Applied Polymer Science, v. 113, p. 2322–2330, 2009. https://doi.org/10.1002/app.30275.

[20] WENDORFF, J.; AGARWAL, S.; GREINER, A. Electrospinning. Materials, Processing, and Applications. Hoboken: Wiley, 2012.

[21] BHARDWAJ, N.; KUNDU, S. C. Electrospinning: A fascinating fiber fabrication technique. Biotechnology Advances, v. 28, n. 3, p. 325–347, 2010. https://doi.org/10.1016/j.biotechadv.2010.01.004.

[22] DARISTOTLE, J. L.; BEHRENS, A. M.; SANDLER, A. D.; KOFINAS, P. A Review of the Fundamental Principles and Applications of Solution Blow Spinning. ACS applied materials & interfaces, v. 8, n. 51, p. 34951-34963, 2016. https://doi.org/10.1021/acsami.6b12994.

[23] SILVA, T. H.; OLIVEIRA, J. E.; MEDEIROS, E. S.; SILVA, T. H.; OLIVEIRA, J. E.; MEDEIROS, E. S. Obtenção de micro e nanofibras de PVC pela técnica de Fiação por Sopro em Solução. Polímeros, v. 25, n. 2, p. 229–235, 2015. https://doi.org/10.1590/0104-1428.1694.

[24] COSTA, R. G. F.; OLIVEIRA, J. E.; PAULA, G. F.; PICCIANI, P. H. S.; MEDEIROS, E. S.; RIBEIRO, C. et al. Eletrofiação de Polímeros em Solução: parte I: fundamentação Teórica. Polímeros, v. 22, n. 2, p. 170–177, 2012. https://doi.org/10.1590/S0104-14282012005000026.

[25] OLIVEIRA, J. E.; MEDEIROS, E. S.; CARDOZO, L.; VOLL, F.; MADUREIRA, E. H.; MATTOSO, L. H. C et al. Development of poly(lactic acid) nanostructured membranes for the controlled delivery of progesterone to livestock animals. Materials Science and Engineering: C, v. 33, n. 2, p. 844–849, 2013. https://doi.org/10.1016/j.msec.2012.10.032.

[26] OLIVEIRA, J. E.; MORAES, E. A.; MARCONCINI, J. M.; C. Mattoso LH, Glenn GM, Medeiros ES. Properties of poly(lactic acid) and poly(ethylene oxide) solvent polymer mixtures and nanofibers made by solution blow spinning. Journal of Applied Polymer Science, v. 129, n. 6, p. 3672–3681. https://doi.org/10.1002/app.39061.

[27] CARRIZALES, C.; PELFREY, S.; RINCON, R.; EUBANKS, T. M.; KUANG, A.; MCCLURE, M. J. et al. Thermal and mechanical properties of electrospun PMMA, PVC, Nylon 6, and Nylon 6,6. Polym Adv Technol v. 19, n. 2, p. 124–130, 2008. https://doi.org/10.1002/pat.981.

[28] MITSUI CHEMICALS. Partícula fina de polietileno de ultra alto peso molecular MIPELON™ 2016. Disponível em: https://www.mitsuichemicalsbrasil.com/mipelon_prop.htm. Acesso em: 5 nov. 2018.

[29] TUTAK, W.; SARKAR, S.; LIN-GIBSON, S.; FAROOQUE, T. M.; JYOTSNENDU, G.; WANG, D. et al. The support of bone marrow stromal cell differentiation by airbrushed nanofiber scaffolds. Biomaterials, v. 34, n. 10, p. 2389–2398. https://doi.org/10.1016/j.biomaterials.2012.12.020.

[30] LI, J.; LUO, K.; YU, J.; WANG, Y.; ZHU, J.; HU, Z. Promising Free-Standing Polyimide Membrane via Solution Blow Spinning for High Performance Lithium-Ion Batteries. Industrial & Engineering Chemistry Research, v. 57, n. 36, p. 12296–12305, 2018. https://doi.org/10.1021/acs.iecr.8b02755.

[31] REIN, D. M.; COHEN, Y.; LIPP, J.; ZUSSMAN, E. Elaboration of Ultra-High Molecular Weight Polyethylene/Carbon Nanotubes Electrospun Composite Fibers. Macromolecular Materials and Engineering, v. 295, n. 11, p. 1003–1008, 2010. https://doi.org/10.1002/mame.201000157.
[32] REIN, D. M.; SHAVIT-HADAR, L.; KHALFIN, R. L.; COHEN, Y.; SHUSTER, K.; ZUSSMAN, E. Electrospinning of ultrahigh-molecular-weight polyethylene nanofibers. Journal of Polymer Science Part B: Polymer Physics, v. 45, n. 7, p. 766–773, 2007. https://doi.org/10.1002/polb.21122.
[33] REIN, D. M.; COHEN, Y.; RONEN, A.; SHUSTER, K.; ZUSSMAN, E. Application of gentle annular gas veil for electrospinning of polymer solutions and melts. Polymer Engineering & Science, v. 49, n. 4, p. 774–782, 2009. https://doi.org/10.1002/pen.21273.
[34] CUI, W.; LI, X.; ZHOU, S.; WENG, J. Investigation on process parameters of electrospinning system through orthogonal experimental design. Journal of Applied Polymer Science, v. 103, n. 5, p. 3105–3112, 2007. https://doi.org/10.1002/app.25464.
[35] PATRA, S. N.; EASTEAL, A. J.; BHATTACHARYYA, D. Parametric study of manufacturing poly(lactic) acid nanofibrous mat by electrospinning. Journal of Materials Science, v. 44, p. 647–654, 2009. https://doi.org/10.1007/S10853-008-3050-Y.
[36] ZONG, X.; KIM, K.; FANG, D.; RAN, S.; HSIAO, B. S.; CHU, B. Structure and process relationship of electrospun bioabsorbable nanofiber membranes. Polymer (Guildf), v. 43, n. 16, p. 4403–4412, 2002. https://doi.org/10.1016/S0032-3861(02)00275-6.
[37] DALTON, P. D.; KLINKHAMMER, K.; SALBER, J.; KLEE, D.; MÖLLER, M. Direct in Vitro Electrospinning with Polymer Melts. Biomacromolecules, v. 7, n. 3, p. 686–690, 2006. https://doi.org/10.1021/BM050777Q.
[38] BOLBASOV, E. N.; ANISSIMOV, Y. G.; PUSTOVOYTOV, A. V.; KHLUSOV, I. A.; ZAITSEV, A. A.; ZAITSEV, K. V. et al. Ferroelectric polymer scaffolds based on a copolymer of tetrafluoroethylene with vinylidene fluoride: fabrication and properties. Materials Science and Engineering: C, v. 40, p. 32–41, 2014. https://doi.org/10.1016/J.MSEC.2014.03.038.
[39] ZHUANG, X.; YANG, X.; SHI, L.; CHENG, B.; GUAN, K.; KANG, W. Solution blowing of submicron-scale cellulose fibers. Carbohydrate polymers, v. 90, n. 2, p. 982–987, 2012. https://doi.org/10.1016/J.CARBPOL.2012.06.031.
[40] SHI L.; ZHUANG, X. P.; CHENG, B. W.; TAO, X. X.; KANG, W. M. Solution blowing of poly(dimethylsiloxane)/nylon 6 nanofiber mats for protective applications. Chinese Journal of Polymer Science, v. 32, p. 786–792. https://doi.org/10.1007/s10118-014-1452-7.
[41] ABDAL-HAY, A.; SHEIKH, F. A.; LIM, J. K. Air jet spinning of hydroxyapatite/poly(lactic acid) hybrid nanocomposite membrane mats for bone tissue engineering. Colloids and Surfaces B: Biointerfaces, v. 102, p. 635–643, 2013. https://doi.org/10.1016/J.COLSURFB.2012.09.017.
[42] THOMPSON, C. J.; CHASE, G. G.; YARIN, A. L.; RENEKER, D. H. Effects of parameters on nanofiber diameter determined from electrospinning model. Polymer, v. 48, n. 23, p. 6913–6922, 2007. https://doi.org/10.1016/J.POLYMER.2007.09.017.
[43] LOU, H.; LI, W.; LI, C.; WANG, X. Systematic investigation on parameters of solution blown micro/nanofibers using response surface methodology based on box-Behnken design. Journal of Applied Polymer Science, v. 130, n. 2, p. 1383–1391, 2013. https://doi.org/10.1002/app.39317.
[44] ZARGHAM, S.; BAZGIR, S.; TAVAKOLI, A.; RASHIDI, A. S.; DAMERCHELY, R. The Effect of Flow Rate on Morphology and Deposition Area of Electrospun Nylon 6 Nanofiber. Journal of Engineered Fibers and Fabrics, v. 7, n. 4, p. 42–49, 2012. https://doi.org/10.1177/155892501200700414.
[45] LI, J.; SONG, G.; YU, J.; WANG, Y.; ZHU, J.; HU, Z. Preparation of Solution Blown Polyamic Acid Nanofibers and Their Imidization into Polyimide Nanofiber Mats. Nanomaterials, v. 7, n. 11, p. 395, 2017. https://doi.org/10.3390/NANO7110395.
[46] OLIVEIRA, J. E.; MATTOSO, L. H. C.; ORTS, W. J.; MEDEIROS, E. S. Structural and Morphological Characterization of Micro and Nanofibers Produced by Electrospinning and Solution Blow Spinning: A Comparative Study. Advances in Materials Science and Engineering, v. 2013, p. 1–14, 2013. https://doi.org/10.1155/2013/409572.